JOURNAL OF GEOPHYSICAL RESEARCH, VOL. 103, NO. A6, PAGES 11,745–11,754, JUNE 1, 1998

Wave characteristics of geomagnetic pulsations across the dip equator

M. Shinohara, K. Yumoto, N. Hosen,[1] A. Yoshikawa, H. Tachihara, O. Saka, and T.-I. Kitamura
Department of Earth and Planetary Sciences, Kyushu University, Fukuoka, Japan

N. B. Trivedi and J. M. Da Costa[2]
Instituto Nacional de Pesquisas Espaciais, São José dos Campos, São Paulo, Brazil

N. J. Schuch
Laboratório de Ciências Espaciais de Santa Maria, Universidade Federal de Santa Maria
Santa Maria, Brazil

Abstract. In order to clarify the wave characteristics of Pi2 and Pc 4-5 magnetic pulsations around the dip equator, we analyzed magnetic data from the latitudinally dense magnetometer array in Brazil. We found that the phase difference between Pi2 pulsations observed at globally separated low-latitude stations is small, whereas Pi2 pulsations observed within the dayside dip equator region of ±2° latitude show phase lags of about 30° ~ 50° behind those in the off-dip equator region. Pc 4-5 magnetic pulsations at the dip equator also show the same phase character. Pi2 amplitudes are enhanced in the equatorial region, where the phase lags of pulsations must be associated with the enhancement of ionospheric conductivity. The equatorial phase lags can be explained by invoking the induction effect of the equatorial enhanced ionospheric current above the good conductor Earth.

1. Introduction

The dip equator is characterized by high zonal ionospheric conductivity. An enhancement of signal amplitude is a general characteristic of geomagnetic phenomena, for example, of the equatorial electrojet (EEJ), *DP* 2, the preliminary reverse impulse (PRI), sudden commencements (sc), sudden impulses (si), Pi2 at the dip equator [cf. *Nishida,* 1968a, b; *Araki,* 1977; *Forbes,* 1981; *Sastry et al.,* 1983; *Itonaga et al.,* 1995; *Sarma and Sastry,* 1995; *Yumoto et al.,* 1996]. Therefore the dip equator is a peculiar region where we can easily observe geomagnetic phenomena.

The EEJ whose localization has been discussed by many researchers, is one of the typical phenomena at the dip equator (for a review, see *Forbes* [1981]). The EEJ current is driven by the Sq field (which is generated by the dynamo in the E region [*Matsushita,* 1967]) and flows in the latitudinally narrow region. Because of inhibition of the vertical current by the relatively low conducting layers, the effective zonal ionospheric conductivity (σ_{yy}) is considerably enhanced near the dip equator [*Sugiura and Cain,* 1966]. Therefore the EEJ current flows strongly in the dip ionosphere, and the large magnetic fluctuation can be observed within a few degrees of latitude on the ground.

Nishida [1968a, b] reported that the *DP* 2 fluctuation appears coherently all over the world. He demonstrated the equatorial enhancement of *DP* 2 variations, whose amplitudes at the equator are several times larger than those at low latitudes.

The PRI associated with storm sudden commencement (ssc) also shows equatorial enhancement. *Araki* [1977] discussed PRI occurrence at the equator as it relates to that at high latitudes. He also compared PRI amplitudes at the dip equator at Koror and at Guam and showed that the rate of equatorial enhancement of PRI became between 2.5 and 4. *Itonaga et al.* [1995] discussed the global structure of low-latitude and equatorial magnetic pulsations associated with ssc. They found a phase delay of ssc-associated geomagnetic pulsations near the dip equator.

Yumoto et al. [1996] found that the amplitudes of sc and si at low and middle latitudes along the 210° magnetic meridian are larger in the summer hemisphere than in the winter hemisphere. They also used the 210°MM data to confirm the enhancement of sc and si amplitudes near the dayside equator.

[1]Now at Hitachi Corporation, Hitachi, Ibaraki, Japan.
[2]Also at Universidade de Taubate, Taubate, São Paulo, Brazil.

Paper number 97JA03067.
0148-0227/98/97JA-03067$09.00

Dayside equatorial and low-latitude Pi2 pulsations have been studied by many authors [*Stuart and Barsczus*, 1980; *Sutcliffe*, 1980; *Sastry et al.*, 1983; *Kitamura et al.*, 1988; *Yumoto et al.*, 1989, 1990; *Sutcliffe and Yumoto*, 1989; *Itonaga et al.*, 1992; *Sarma and Sastry*, 1995]. They have discussed the relationships of dayside Pi2 to nightside substorms, longitudinal extent, and amplitude enhancement at the equator. *Sastry et al.* [1983] showed the local time variation of the amplitude ratio of the equatorial enhancement. The amplitude ratio was found to vary between 1.4 and 3.5 for daytime events, and the mean ratio reached a maximum of 2.3 at noon. Recently, *Sarma and Sastry* [1995] demonstrated the dependence of equatorial enhancement on the period and type of geomagnetic variations. They classified various types of geomagnetic phenomena, from geomagnetic fluctuations with long periods (T is approximately a few minutes to 1 h) to pulsations with very short periods ($T < 20$ s), and showed that amplitude enhancement amounted to 2.0–2.5 over a wide range of time periods and that there was a sharp cutoff of the enhancement at a period of around 20 s.

Detailed analyses of magnetic pulsations around the dip equator region were mainly of amplitude enhancement, whereas it is rarely studied in the phase relation, because the time accuracy of magnetic data obtained around the equator was insufficient for the comparison of signals between separated stations. In combination with high time resolution and accurate time data from the magnetic equator [*Tachihara et al.*, 1996] and the 210° magnetic meridian networks [*Yumoto and the 210° MM Magnetic Observation Group*, 1996], we are recently able to investigate phase and amplitude relationships across the dip equator.

In this paper, we demonstrate the peculiar phase relationship of Pi2 and Pc 4-5 pulsations across the dip equator and suggest the importance of the induction effect of the localized ionospheric current at the dip equator.

2. Observation and Data

The magnetometer data used here were taken from two Brazilian arrays: the east coast array at São Luís (SLZ; geographic latitude $\lambda = -2.60°$, geographic longitude $\phi = -44.20°$, dip latitude = 0.3°), Teresina (TER; −5.03°, −42.83°, −2.5°), Eusebio (EUS; −3.85°, −38.42°, −3.8°), Cachoeira Paulista (CPA; −22.69°, −45.01°, −16.6°), and Santa Maria (SMA; −29.72°, −53.72°, −19.8°) and the Rondônia array at Pôrto

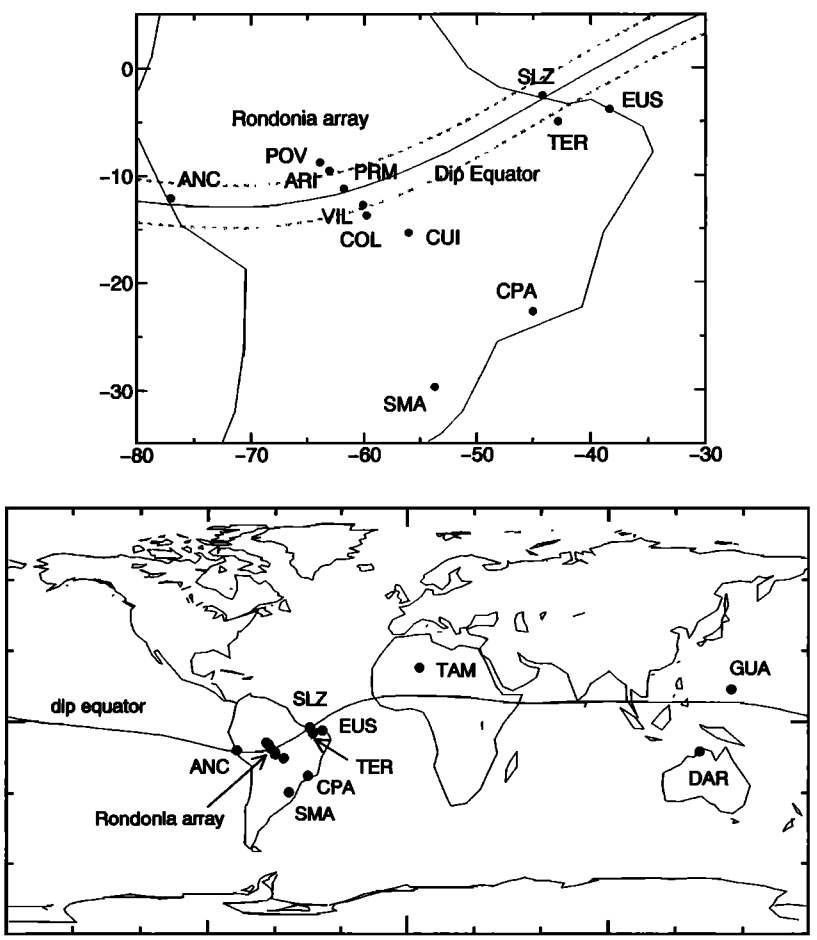

Figure 1. Locations of stations on the Brazilian east coast and in the (a) Rondônia array and of the (b) other low-latitude stations used in this study. Solid and broken lines indicate the dip equator and the schematic extent of the equatorial electrojet current (±2°), respectively.

Table 1. Coordinates of Stations

Station Name	Abbreviation	Geographic		Geomagnetic		L	I[a]	Dip Latitude[b]
		Latitude	Longitude	Latitude	Longitude			
1992								
São Luís	SLZ	−2.60	−44.20	0.94	29.51	1.00	0.22	0.3
Teresina	TER	−5.03	−42.83	−1.23	29.57	1.00	−5.74	−2.5
Eusebio	EUS	−3.85	−38.42	0.21	34.66	1.00	−8.85	−3.8
Cachoeira Paulista	CPA	−22.69	−45.01	−16.11	21.60	1.08	−30.77	−16.6
Santa Maria	SMA	−29.72	−53.72	−18.95	13.19	1.12	−32.70	−19.8
Ancón	ANC	−12.08	−77.02	1.50	354.41	1.00	1.13	0.5
Tamanrasset	TAM	22.80	5.53	5.93	78.28	1.05	27.81	10.5
Guam	GUA	13.58	144.87	5.61	215.40	1.01	11.53	5.6
Darwin	DAR	−12.43	130.83	−22.07	202.57	1.16	−40.95	−20.6
1995								
Pôrto Velho	POV	−8.80	−63.90	2.66	7.63	1.00	5.57	3.0
Ariquemes	ARI	−9.56	−63.04	1.72	8.36	1.00	3.76	2.0
Presidente Medice	PRM	−11.20	−61.80	0.57	9.41	1.00	0.11	0.0
Vilhena	VIL	−12.72	−60.13	−1.84	10.60	1.00	−3.63	−1.9
Colibri	COL	−13.70	−59.80	−2.87	10.72	1.00	−5.59	−2.9
Cuiabá	CUI	−15.35	−56.05	−5.68	13.83	1.01	−11.12	−5.8

[a]Magnetic inclination.
[b]Dip latitude is defined as the geocentric angle that corresponds to the distance from the dip equator.

Velho (POV; −8.80°, −63.90°, 3.0°), Ariquemes (ARI; −9.56°, −63.04°, 2.0°), Presidente Medice (PRM; −11.20°, −61.80°, 0.0°), Vilhena (VIL; −12.72°, −60.13°, −1.9°), Colibri (COL; −13.70°, −59.80°, −2.9°), and Cuiabá (CUI; −15.35°, −56.05°, −5.8°), as shown in Figure 1. These Brazilian array projects were conducted by T.-I. Kitamura, Kyushu University, during the interval 1988–1995. Magnetic field data from the east coast array and from the Rondônia array are available during the intervals from December 1988 to March 1995, and from September 1993 to January 1995, respectively. Data from four equatorial and low-latitude stations at Ancón (ANC; −12.08°, −77.02°, 0.5°), Tamanrasset (TAM; 22.80°, 5.53°, 10.5°), Guam (GUA; 13.58°, 144.87°, 5.6°), and Darwin (DAR; −12.43°, 130.83°, −20.6°) were also used to clarify the global behavior of Pi2 pulsations. Part of these stations are distributed globally and the others are distributed to be locally dense near the equator in order to investigate the global and localized nature of magnetic pulsations. Geographic and geomagnetic coordinates of the stations are listed in Table 1.

Fluxgate magnetometers [*Tachihara et al.*, 1996] with a self-time calibration system were installed. The data were digitized with 3-s sampling. The clock of the data logger was calibrated automatically by HF standard time signals [*Saka and Tachihara*, 1986] or LF OMEGA signals [*Saka et al.*, 1996]. The time accuracy was kept to within 100 ms during the observed period.

3. Characteristics of Equatorial and Low-Latitude Pi2 Pulsations

The wave characteristics of Pi2 magnetic pulsations at the dip equator and low latitudes are clarified in this section. We show two examples of Pi2 events observed at nine stations (SLZ, TER, EUS, CPA, SMA, ANC, TAM, GUA, and DAR) distributed globally from the dayside to the nightside as shown in Figure 1b. The first and second events occurred when the Brazilian east coast array was located on the nightside and the dayside, respectively.

The first event occurred at 2215 UT on June 29, 1992. The top of Figure 2 shows the H component magnetic variation observed at the nightside low-latitude station SMA (LT = UT−3.6 hours, dip latitude = −19.8°) during the time interval 2145–2245 UT. A substorm-associated bay variation can be seen at the center of the magnetic record. The bottom plots in Figure 2 show bandpass-filtered (40–150 s) data for H component magnetic variations observed at the equatorial and low-latitude stations ANC (LT = UT−5.1 hours, dip latitude = 0.5°), SMA (UT−3.6 hours, −19.8°), SLZ (UT−2.9 hours, 0.2°), TAM (UT+0.4 hours, 10.5°), DAR (UT+8.7 hours, −20.6°), and GUA (UT+9.7 hours, 5.6°). At that time, ANC, and SLZ and SMA were located in the dusk sector at LT ~ 1715 and LT ~ 1930, respectively. TAM was located near the midnight (LT ~ 2245), while DAR (LT ~ 0700) and GUA (LT ~ 0800) were located in the dawn sector. Although waveforms of Pi2 magnetic pulsations at 2203 and 2215 UT are a little bit different at the globally separated stations, Pi2 pulsations show a globally concurrent appearance from night to day [cf. *Kitamura et al.*, 1988; *Sutcliffe and Yumoto*, 1989].

In order to see the latitudinal phase relation of Pi2 pulsations near the dip equator, expanded amplitude-time records from the Brazilian array stations at SLZ, TER(UT−2.9 hours, −2.5°), EUS(UT−2.6 hours, −3.8°), CPA(UT−3.0 hours, −16.6°), and SMA (see Figure 1a) in the interval from 2213 to 2221 UT are shown in Figure 3. In this event, the Brazilian array

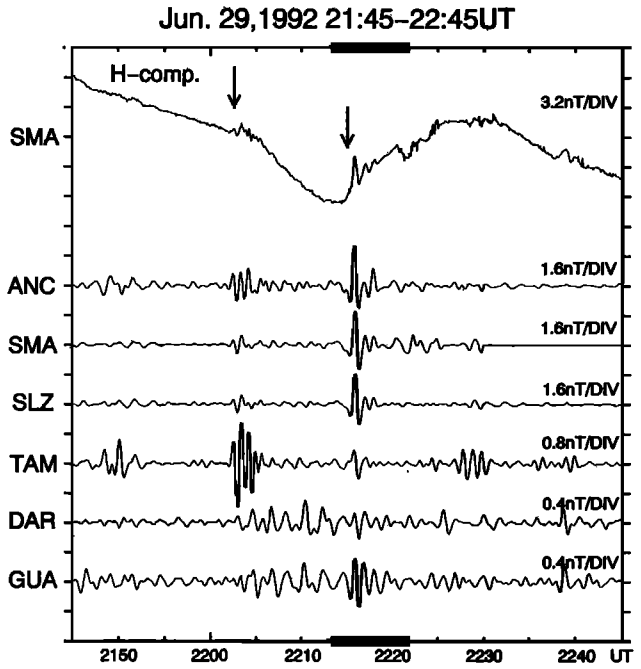

Figure 2. H component magnetograms observed at six globally distributed stations SMA (λ = −29.72°, ϕ = −53.72°), ANC (−12.08°, −77.02°), SLZ (−2.60°, −44.20°), TAM (22.80°, 5.53°), DAR (−12.43°, 130.83°), and GUA (13.58°, 144.87°) during the period from 2145 to 2245 UT on June 29, 1992. The magnetograms have been bandpass filtered between 40 and 150 s, except for the top one. The arrows indicate the onset times of Pi2 associated with magnetic substorms.

was located around 1930 LT. Similar waveforms can be identified at all the stations. The vertical lines in Figure 3 are drawn for comparison of the phase difference between Pi2 pulsations at different stations. No phase lag in Pi2 pulsations from the dip station (SLZ) to the low-latitude station (SMA) can be seen in the dusk sector.

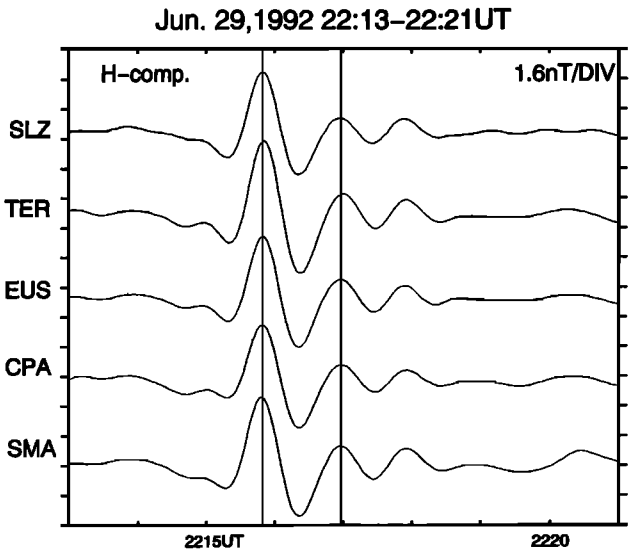

Figure 3. Expanded amplitude-time records from the Brazilian east coast array SLZ (dip latitude is 0.3°), TER (−2.5°), EUS (−3.8°), CPA (−16.6°), and SMA (−19.8°) for the period from 2213 to 2221 UT.

The second event occurred at 1316 UT on June 20, 1992. The H component magnetic variation during the time interval 1245–1345 UT at the nightside low-latitude station DAR is shown at the top of Figure 4. A magnetic bay variation can be seen at the center of Figure 4. The bottom plots show bandpass-filtered (40–150 s) data from the six equatorial and low-latitude stations. At that time, ANC was located in the dawn sector (LT ~ 0815). The stations at SLZ and SMA, and at TAM were located in the prenoon (LT ~ 1030) and postnoon (LT ~ 1345) sectors, respectively. DAR (LT ~ 2200) and GUA (LT ~ 2300) were located in the nighttime sector. Even though Pc 4 magnetic pulsations are activated during local daytime at ANC, SMA, and SLZ, the amplitude-time records show corresponding clear Pi2 oscillations at 1315 UT. This is very similar to what occurred during the previous event.

Expanded amplitude-time records from 1314 to 1322 UT are shown in Figure 5. In this case, the Brazilian array was located around 1030 LT. Phase differences of Pi2 pulsations at SMA, CPA, and EUS are small, whereas considerable phase lags can be recognized between the dip equator stations at SLZ and TER and the other off-dip stations. The phase lag increases gradually from EUS to TER and SLZ. The time lag between SLZ and the off-dip stations (EUS, CPA, and SMA) is about 6 s. The phase lag between equatorial Pi2 and low-latitude Pi2 can be seen in the prenoon sector of ~ 1030 LT.

According to statistical results shown in the followings, the phase lag at the dip equator is not due to contamination of other pulsation activities.

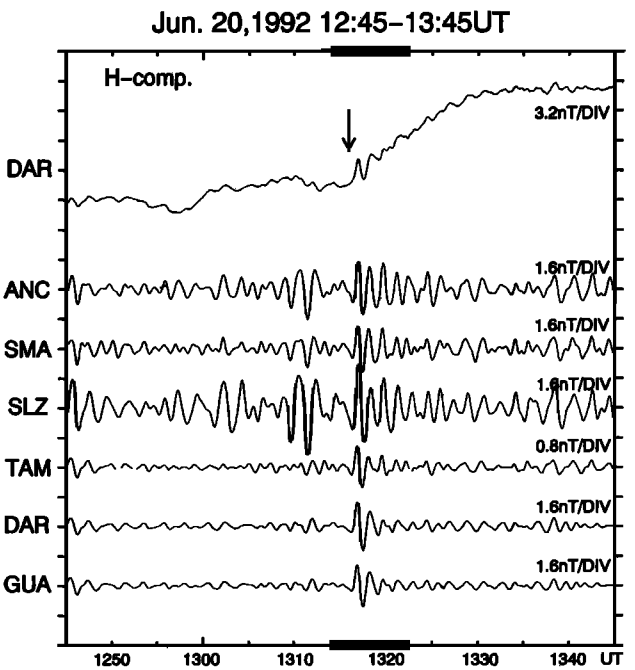

Figure 4. H component magnetograms observed at six globally distributed stations SMA, ANC, SLZ, TAM, GUA, and DAR during the period from 1245 to 1345 UT on June 20, 1992. The magnetograms have been bandpass filtered between 40 and 150 s, except for the top one. The arrow indicates the onset time of Pi2.

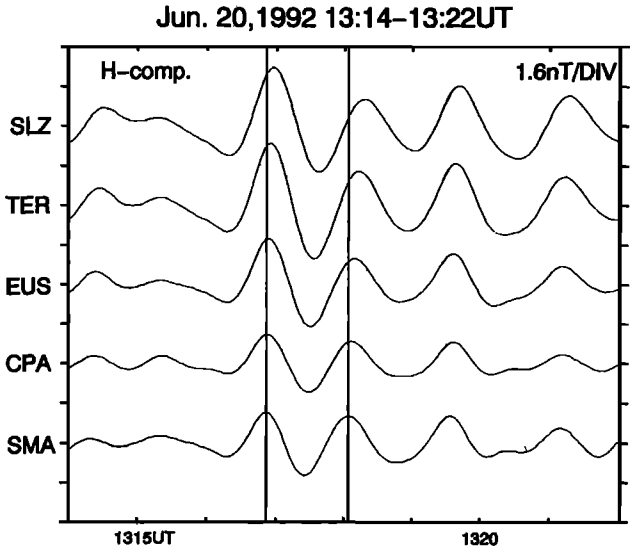

Figure 5. Expanded amplitude-time records from the Brazilian east coast array SLZ, TER, EUS, CPA, and SMA for the period from 1314 to 1322 UT.

3.1. Phase Relation of Pi2 at the Dip Equator

In order to clarify the dependence of phase lag of an equatorial Pi2 on local time and dip latitude, we statistically analyzed 107 Pi2 events observed from June 1, 1992, to July 5, 1992, at the Brazilian east coast array. The diurnal changes in the phase difference between a pair of stations (TER (dip latitude = −2.5°)–SLZ (0.3°), EUS (−3.8°)–SLZ, and SMA (−19.8°)–SLZ) were obtained by using the cross-correlation function.

The phase lags of Pi2 pulsations between TER–SLZ, EUS–SLZ, and SMA–SLZ are shown as a function of local time in Figure 6. A positive (negative) sign is assigned to the phase lag if the signal at the former station lags (leads) that at the other station. Figure 6a shows the phase lags of Pi2 pulsations between dip equator station SLZ (dip latitude is 0.3°) and near-equator station TER (−2.5°) as a function of local time. The phase lags of Pi2 pulsations observed near the dip equator are small during the entire day. Significant phase lags appear between SLZ and EUS (−3.8°), as shown in Figure 6b. A local time dependence of phase lags can be seen in this figure. The phase of Pi2 at SLZ lags that at EUS when the stations are on the dayside. The averaged phase lag during local daytime (0800–1600 LT) is −28°. On the other hand, the phase lag is small when the stations are on the nightside. The averaged phase lag during local nighttime (2000–0400 LT) is −9°. Figure 6c shows the phase lag of Pi2 between SLZ and SMA. SMA (−19.8°) is the station farthest south, in this array. Although the plots are more scattered, Figure 6c shows the same trend as Figure 6b. The averaged phase lag during the local daytime is −44°, while that during the local nighttime is −16°. Though negative deviations are also seen in the predawn sector, it will be re-examined in detail and presented in the future paper whether these deviations are significant or not.

We conclude that the phase lag of Pi2 pulsations is most lagged at the dip equator. With increasing of the dip latitude, the phase lag is gradually decreasing.

3.2. Equatorial Enhancement of Pi2 Amplitudes

Sastry et al. [1983] and *Sarma and Sastry* [1995] examined the local time dependence of amplitude enhancement of the pulsation signal at the dip equator. In order to discuss the relationship between amplitude enhancement and phase lag in the equatorial region, the amplitude ratios between the dip station and off-dip stations were plotted as a function of local time in Figure 7.

Figure 7a shows the ratio of Pi2 amplitudes observed at the Brazilian east coast array at SLZ (dip latitude is 0.3°) to those observed at TER (−2.5°). The amplitude ratio was distributed at ~ 1 during the entire day. Figure 7b shows the ratio of Pi2 amplitudes at SLZ to those at EUS (−3.8°). The amplitude ratio becomes ~ 1 during local nighttime, whereas the averaged ratio reaches 1.5 during local daytime. Figure 7c shows the ratio of Pi2 amplitudes at SLZ and SMA (−19.8°).

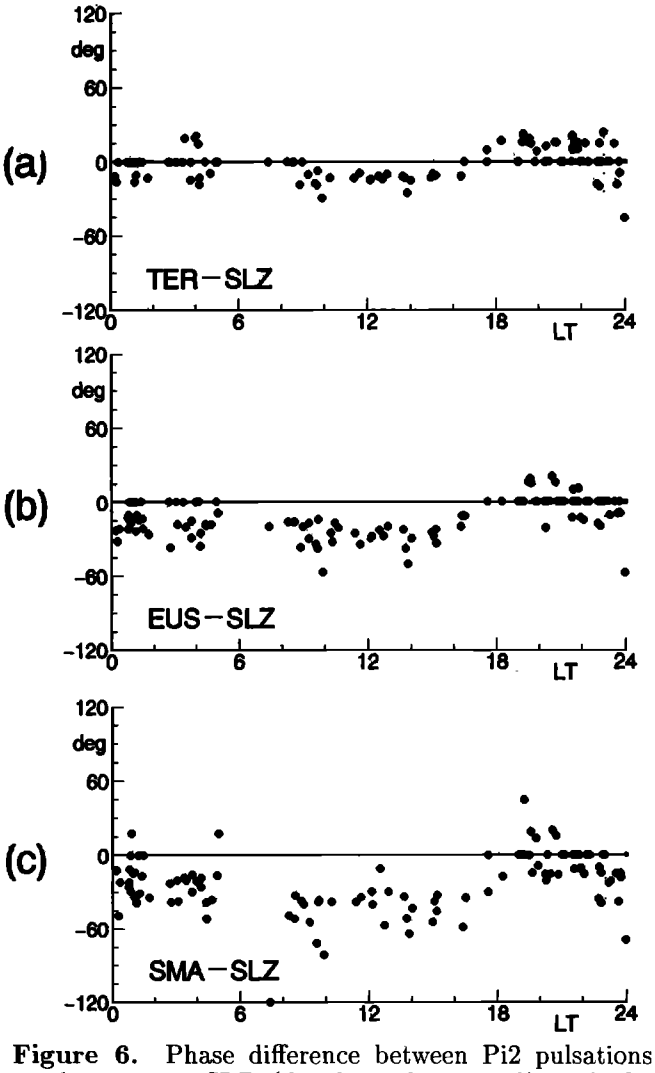

Figure 6. Phase difference between Pi2 pulsations at dip station SLZ (dip latitude is 0.3°) and the other Brazilian east coast stations TER (−2.5°), EUS (−3.8°), and SMA (−19.8°) as a function of local time.

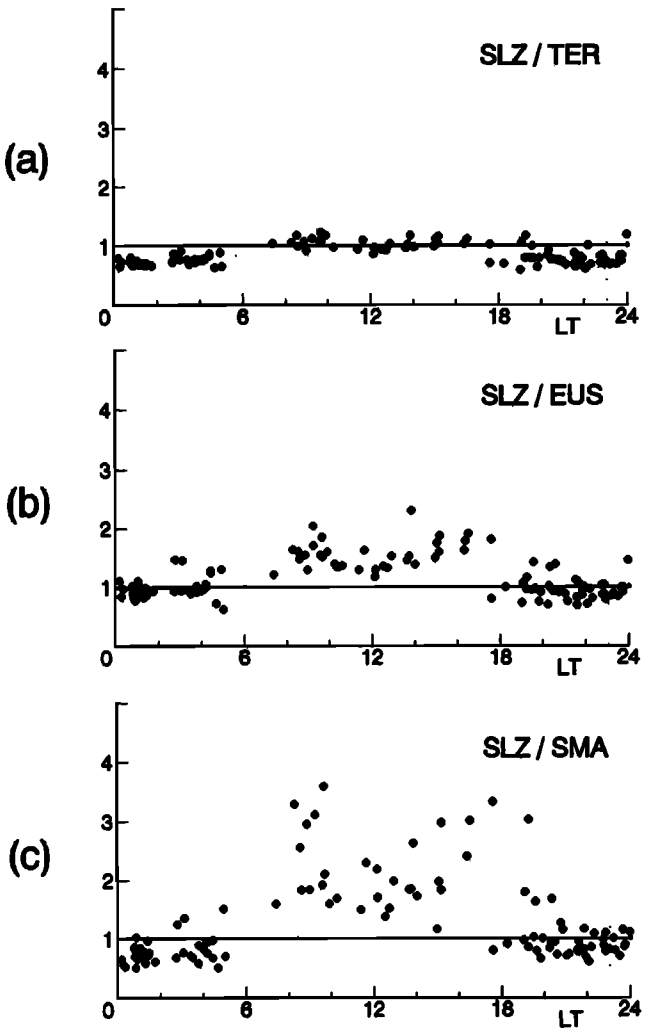

Figure 7. Amplitude ratios of Pi2 pulsations between dip station SLZ and the other Brazilian east coast stations TER, EUS, and SMA as a function of local time.

The plots of SLZ–SMA are more scattered than those of SLZ–EUS, with increasing the distance between the stations. The amplitude enhancement of equatorial Pi2 can be reconfirmed during local daytime. The averaged ratio of Pi2 amplitudes at SLZ–SMA is 2.1.

In summary, the amplitude ratio of Pi2 increases as one approaches the dip equator, a trend that is similar to that of phase lags of equatorial Pi2, as shown in the previous section.

4. Phase Relations of Pc 4-5 Pulsations

Usually, Pc 4-5 magnetic activities are believed to be intensified during local daytime at the equator, i.e., similarly to the equatorial enhancement of Pi2 [*Sarma and Sastry,* 1995]. If the phase lag of equatorial Pi2 is associated with the equatorial enhancement of Pi2 amplitudes, then one would expect Pc 4-5 pulsations at the dip equator to also lag those in the off-dip equator region. We applied fast Fourier transform analysis to the data set to clarify daily variations of phase lags of Pc 4-5 pulsations around the dip equator. The data used here are from the Rondônia array in Brazil, which is a latitudinally dense array that crosses the dip equator, as shown in Figure 1a. The structure of the phase lags is discussed in more detail below.

Figure 8 shows the phase relationships of magnetic pulsations between dip station PRM (dip latitude = 0.0°) and stations POV (3.0°), ARI (2.0°), VIL (−1.9°), COL (−2.9°), and CUI (−5.8°) as a function of wave frequency and local time. The phase differences between two stations are shown in the gray scale. Gray means that the phase difference is very small. If the signal at the dip station lags that at the other station, the shades are dark gray and black. Light gray and white represent that the signal at the dip leads the other. The plots of power spectra in the figure are displayed when the pulsation power at PRM are higher than 3.8×10^{-9} nT^2/Hz. The flat light gray shade in the frequency-time diagrams corresponds to the nonactivity of pulsations.

Stations ARI and VIL are located close to the dip equator on its northern and southern sides, that is, 2° north and south, respectively. With respect to daily variations in the magnetic field at ARI and VIL, the EEJ current flows near these stations. Therefore ARI and VIL are still located within the daytime conductivity enhancement region. Figures 8b and 8c show the phase differences between ARI and PRM and between VIL and PRM, respectively. Both panels show gray during the entire day of September 24, 1994, indicating that the pulsations at PRM are in phase with those at ARI and VIL in the daytime and also in the nighttime.

Figure 8e shows the phase difference between dip station PRM and station CUI, which is the station in the Rondônia array most distant (5.8° south) from the dip. During the nighttime (from 1800 to 0600 LT), gray is predominant in the whole frequency range. Therefore the phase difference becomes small at night. On the other hand, the shade is dark gray during the daytime (from 0600 to 1800 LT). The signal at dip station PRM lags that at low-latitude station CUI in the daytime. The dominant phase difference of pulsations in the frequency range between 5 and 20 mHz (correspond to Pc 4) is about 30°–40°. It is also noteworthy that pulsations in the frequency range lower than 5 mHz show a shade intermediate between gray and dark gray (approximately 20°). The phase difference between PRM and CUI depends on wave frequency.

Stations POV and COL are located at 3° north and south, respectively, from the dip equator; i.e., they are the stations latitudinally intermediate between VIL and CUI. Figures 8a and 8d show no phase difference between the dip and these stations during the night. Magnetic pulsations in the frequency range higher than 5 mHz show a shade intermediate between gray and dark gray (10°–20°). The equatorial phase lag can be recognized in this latitude, but the lag is smaller than that at PRM–CUI. Equatorial pulsations in the frequency range lower than 5 mHz show gray; that is, there is no phase lag. This result is consistent with the previous phase relation, which is dependent on the wave frequency, as shown in Fig. 8e.

In summary, the phase lags of Pc 4-5 pulsations have

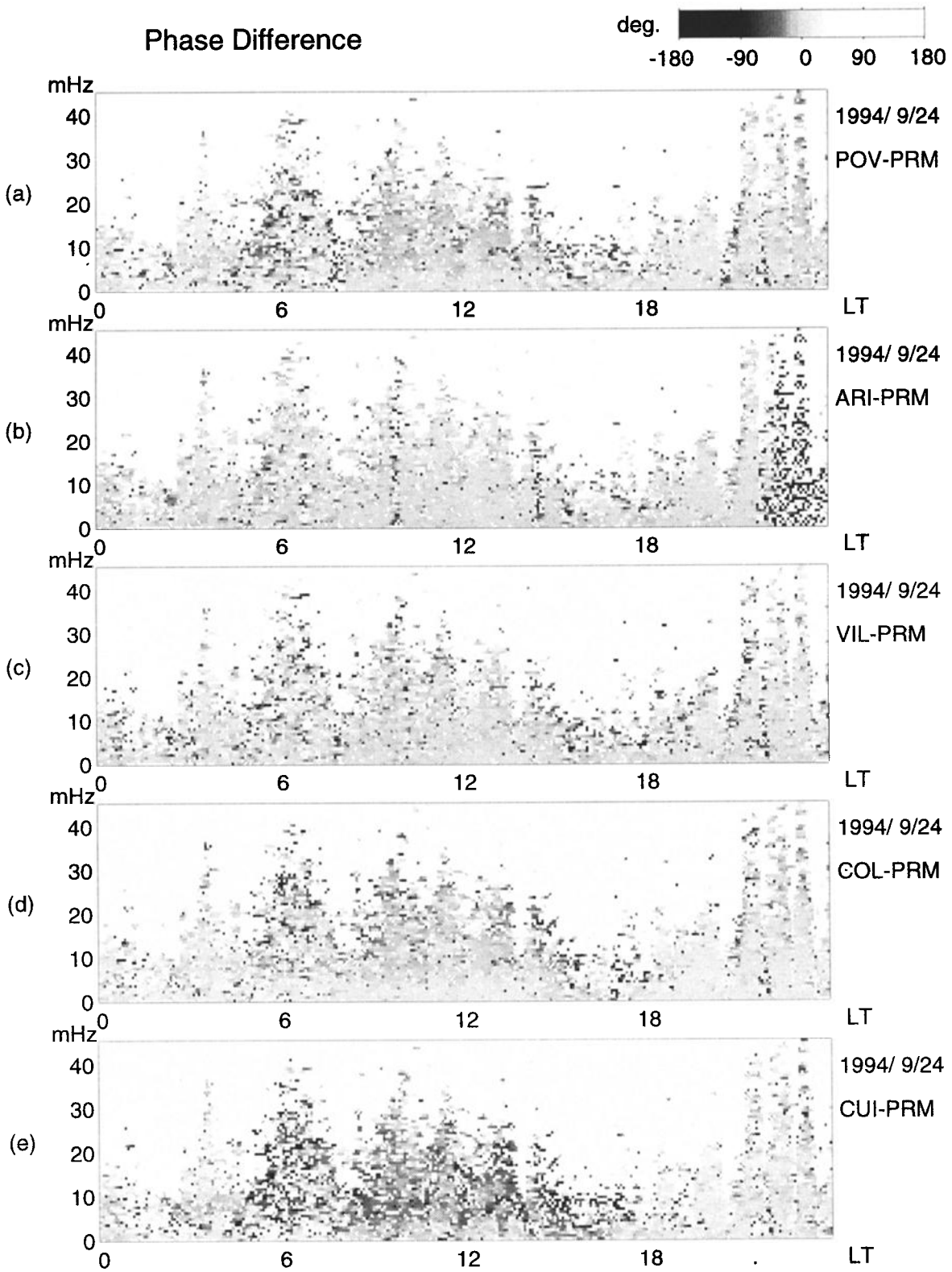

Figure 8. Phase relationships of magnetic pulsations at dip station PRM (dip latitude = 0.0°), and the other Rondônia stations POV (3.0°), ARI (2.0°), VIL (−1.9°), COL (−2.9°), and CUI (−5.8°) as a function of wave frequency and local time.

been identified across the dip equator during the local daytime. The phase lags depend on the wave frequency; that is, equatorial pulsations with higher frequencies show larger phase lags.

5. Summary and Discussion

In this paper, we have analyzed magnetic field data from the Brazilian arrays and from four globally separated stations to clarify daily variations in phase and amplitude relationships of magnetic pulsations between dip and off-dip stations. We can summarize the results as follows:

1. Pi2 pulsations show a globally concurrent appearance from night to day in the equatorial and low-latitude regions.

2. The phase of Pi2 pulsations at the dip equator lags that at low latitudes during local daytime. The averaged phase lag during the daytime at the dip station is 28° behind that at the 3.8° dip latitude station and 44° behind that at the 19.8° dip latitude.

3. The amplitude enhancement of equatorial Pi2 can be reconfirmed during the daytime. The averaged ratio of Pi2 amplitudes at the dip station to those at the 3.8° dip latitude station is 1.5, and the ratio to those at the 19.8° dip latitude is 2.1.

4. The phase lags of Pc 4-5 pulsations are seen across the dip equator during the daytime, similar to equatorial Pi2 pulsations. The averaged phase difference between the dip station and the 5.8° dip latitude station is about 30°–40° for pulsations in the frequency range between 5 and 20 mHz and about 20° for the frequency range lower than 5 mHz. Phase lags increase with increasing wave frequency.

The equatorial ionosphere is characterized by a large latitudinally localized zonal conductivity (σ_{yy}). Ionospheric conductivity depends on local time, and the equatorial large σ_{yy} appears only during the daytime. It is expected that this high conductive ionosphere affects the incident electromagnetic signal. Because the phase lags of equatorial pulsations appear during the daytime, the phase lags must be related to the high ionospheric conductivity.

We suggest a simple model to explain the phase lag of Pi2 pulsations at the dayside dip equator. The ionospheric current generates the magnetic field above and below the ionosphere. The ionosphere is located above the good conductor Earth, and the dielectric region of atmosphere is surrounded with these two good conducting layers. Due to the shielding effect by the Earth current, the magnetic field generated below the ionosphere is confined among the ionosphere and the Earth. The time-varying magnetic field confined in the atmosphere can induce the considerable secondary electric field in the ionosphere by Faraday's law. Then the secondary ionospheric current can be generated. The strength of the secondary ionospheric current depends on the ionospheric conductivity. Therefore, this induction effect associated with the configuration of ionosphere–atmosphere–Earth layers becomes an important role at the dip equator, although it is generally neglected in ULF studies.

ULF phase lags observed at the dayside dip equator indicate the possibility of the coupling between the ionosphere and the Earth. In order to examine it strictly, wave equations in the ionosphere–atmosphere–Earth region should be used and be solved. However the wave equations are not simple [e.g., *Itonaga et al.*, 1997], therefore we present the coupling by using the simplified model in this paper. It may be simplified too much, but, it is a valuable analysis of the equatorial phase lag as the initial discussion. A more detailed analysis will be presented in the future paper.

We assume the good conducting ionosphere at the dip equator as a electric line above the Earth, because the ionospheric current at the dip equator is latitudinally narrow and is extending in longitude. The line above the good conductor Earth have some inductance L which depend on the situation of the line and the Earth. The line also have some resistance R. Therefore the line can be compared with a LR circuit. When an alternating electric field imposes on the line, the current in the line lags to the alternating electric field. The phase lag is represented by

$$\phi = \tan^{-1}\left(-\frac{L\omega}{R}\right).$$

To estimate briefly the phase lag ϕ, we calculate the inductance of the localized ionospheric current system. The inductance L (H) of a line current above the perfect conducting Earth is given by

$$L = \frac{l}{2\pi}\left(\mu_0 \log\frac{2h}{d} + \frac{\mu}{4}\right),$$

where d, l, and h are the radius, length, and height of the line current, respectively. μ and μ_0 denote the magnetic permeability of the ionosphere and vacuum, respectively. *Sugiura and Poros* [1969] showed the cross section of σ_{yy} distribution for longitude 280° E in the daytime. According to their figure, the region of the large σ_{yy} is estimated as approximately 2.0×10^5 m wide, 1.5×10^4 m thick, and 1.0×10^5 m high at the center. Notice that the large-σ_{yy} limit is defined as 5.0×10^{-3} mho/m. Furthermore, to simplify the estimation of inductance L, it is assumed in this study that the high-conductivity region is a section of a circle with a radius of 3.0×10^4 m whose area is comparable to that determined previously. Substitute the defined value, and $\mu = \mu_0$

$$L = 4.3 \times 10^{-7} \times l.$$

This estimation is for daytime conditions. The average value of σ_{yy} is assumed to be 7.5×10^{-3} mho/m; then resistance R (Ω) is determined as

$$R = 4.7 \times 10^{-8} \times l.$$

By using derived L and R, ϕ becomes

$$\phi = \tan^{-1}\left(-\frac{L\omega}{R}\right) = \tan^{-1}(-9.1\omega).$$

ϕ of Pi2 pulsations with dominant period of 60–120 s is estimated as

$$\phi = -43° \sim -25°.$$

On the other hand, R becomes 1 order larger at the off-dip equator region. Then ϕ is estimated as

$$\phi = -5.4° \sim -2.7°.$$

As a result, Pi2 pulsations observed at the dip equator lag to those observed at the off-dip latitudes. Estimated phase differences are comparable to those observed during the daytime (see observational result 2 above). During the nighttime, the ionospheric conductivity at the dip equator is still relatively enhanced to those at the off-dip latitudes, however, the ionospheric conductivity is reduced to about 1/100 of that in the daytime. On the other hand, L is independent of the local time. Therefore, the phase lag given by $\phi = \tan^{-1}(-L\omega/R)$ becomes quite small.

Note that if a longer period is substituted in this equation, the phase difference becomes small, a result that is consistent with result 4.

Our model calculation is quite a simple estimation. A more detailed and accurate estimation would be needed to confirm the observational results.

Some mechanisms of the incidence of the electric field in the equatorial ionosphere were considered by a number of authors. *Araki* [1977] analyzed the coincident occurrence of the PRI at afternoon high-latitude region and at the dayside equator. The PRI appears almost simultaneously with similar waveforms in both the dayside equatorial and the afternoon high-latitude regions, and the equatorial enhancement of PRI is larger than that of the main impulse. Then Araki interpreted that the polar electric field causes the polar PRI and the equatorial PRI. *Kikuchi* [1986] showed schematically that the westward electric field produced by the compression of the magnetosphere is transmitted to the polar ionosphere by the Alfvén mode wave. Then the polar electric field is further transmitted instantaneously to the equator [*Kikuchi et al.*, 1978; *Kikuchi and Araki*, 1979]. The electric field decreases monotonically with decreasing latitude, but the electric current increases abruptly because of conductivity enhancement at the daytime dip equator and makes a significant contribution to geomagnetic variations there.

As demonstrated result 3 above, the amplitude enhancement of Pi2 at the daytime dip equator is similar to that of the PRI. If it is assumed that the daytime equatorial Pi2 is caused by the instantaneous transmission of the polar electric field, it is possible to interpret the phase lags of Pi2 at the dip equator by invoking the previous model calculation.

Yumoto et al. [1989] represented a possible scenario for the excitation of low-latitude Pi2. They assumed that MHD waves are launched at the time of field dipolarization in the near-Earth tail. The compressional portion of the MHD disturbance propagates across the equatorial magnetic field. Then a cavity-resonance-like mode of the plasmasphere is excited. On the other hand, some disturbance can propagate along the field line in the Alfvén mode to the high-latitude ionosphere.

At that time, it is possible that a Pi2-associated electric field in the magnetosphere can be impressed on the polar ionosphere and transmitted instantaneously to the dayside low-latitude region and the equatorial ionosphere. Then Pi2 magnetic pulsations can be observed in the dayside equatorial region.

Takahashi et al. [1992] studied Pi2 pulsations whose waveforms match those of Pi2 pulsations simultaneously observed on the ground at Kakioka ($L = 1.2$), in the inner magnetosphere ($L = 2 \sim 5$), by using AMPTE CCE satellite magnetic data. They found 25 Pi2 events which had all but one been observed within ±3 hours of midnight in the inner magnetosphere.

It is very interesting that no Pi2 pulsation was observed in the dayside magnetosphere. Although the compressional Pi2 waves generated in the nightside magnetosphere can propagate to the dayside magnetosphere, these waves must be not observed in the dayside inner magnetosphere because of the attenuation of the wave energy. Therefore the dayside Pi2 on the ground may be associated with the polar electric field rather than the compressional wave from the magnetosphere. Further observational studies are necessary to clarify the similarity and concurrency of Pi2 magnetic pulsations at the dayside equator and the nightside high and low latitudes.

Moreover, we demonstrated the similarity of the equatorial phase lags of Pi2 and Pc 4-5 pulsations, although the phase lags of Pc5 are less than those of Pi2. We propose that the same transmission mechanism of the polar electric field into the dayside low latitude and equatorial regions may be available for Pi2 and Pc 4-5 magnetic pulsations.

Acknowledgments. We are grateful to M. Itonaga of Yamaguchi University for his useful discussion. We are grateful to M. Ishitsuka of the Instituto Geofísico del Perú and P. Hattori of the U.S. Geological Survey for their kind maintenance of the Ancón and Guam magnetometers, respectively, and B. J. Fraser of the University of Newcastle for his contribution to the operation of the Darwin magnetometer. We also thank F. Ogura and M. Okada of INPE for invaluable help with the setting of magnetometers in the Brazilian arrays.

The Editor thanks P. K. Sutcliffe, M. J. Engebretson, and another referee for their assistance in evaluating this paper.

References

Araki, T., Global structure of geomagnetic sudden commencements, *Planet. Space Sci., 25*, 373, 1977.

Forbes, J. M., The equatorial electrojet, *Rev. Geophys., 19*, 469, 1981.

Itonaga, M., T.-I. Kitamura, O. Saka, H. Tachihara, M. Shinohara, and A. Yoshikawa, Discrete spectral structure of low-latitude and equatorial Pi 2 pulsation, *J. Geomagn. Geoelectr., 44*, 253, 1992.

Itonaga, M., K. Matsuzono, T.-I. Kitamura, I. Toshimitsu, N. B. Trivedi, R. Horita, T. Watanabe, and J. Riddick, Global structure of low-latitude and equatorial geomagnetic pulsations associated with storm sudden commencements, *J. Geomagn. Geoelectr., 47*, 441, 1995.

Itonaga, M., A. Yoshikawa, and K. Yumoto, Transient re-

sponse of the non-uniform equatorial ionosphere to compressional MHD waves, *J. Atmos. Solar Terr. Phys.*, in press, 1997.

Kikuchi, T., Evidence of transmission of polar electric fields to the low latitude at times of geomagnetic sudden commencements, *J. Geophys. Res., 91,* 3101, 1986.

Kikuchi, T., and T. Araki, Horizontal transmission of the polar electric field to the equator, *J. Atmos. Terr. Phys., 41,* 927, 1979.

Kikuchi, T., T. Araki, H. Maeda, and K. Maekawa, Transmision of polar electric fields to the equator, *Nature, 273,* 650, 1978

Kitamura, T.-I., O. Saka, M. Shimoizumi, H. Tachihara, T. Oguchi, T. Araki, N. Sato, M. Ishitsuka, O. Veliz, and J. B. Nyobe, Global mode of Pi 2 waves in the equatorial region — Difference of Pi 2 mode between high and equatorial latitudes, *J. Geomagn. Geoelectr., 40,* 621, 1988.

Matsushita, S., Solar quiet and lunar daily variation fields, in *Physics of Geomagnetic Phenomena,* edited by S. Matsushita and W. H. Campbell, Academic, San Diego, Calif., 1967.

Nishida, A., Geomagnetic D_P2 fluctuations and associated magnetospheric phenomena, *J. Geophys. Res., 73,* 1795, 1968a.

Nishida, A., Coherence of geomagnetic D_P2 fluctuations with interplanetary magnetic variations, *J. Geophys. Res., 73,* 5549, 1968b.

Saka, O., and H. Tachihara, A compact magnetometer data acquisition system with accurate chronometer, *J. Geomagn. Geoelectr., 38,* 221, 1986.

Saka, O., M. Shinohara, H. Tachihara, H. Akaki, H. Inoue, T. Uozumi, and T. Kitamura A time source for a data acquisition system designed for phase propagation study of magnetic pulsations *J. Geomagn. Geoelectr., 48,* 1321-1326, 1996.

Sarma, S. V. S., and T. S. Sastry, On the equatorial electrojet influence on geomagnetic pulsation amplitudes, *J. Atmos. Terr. Phys., 57,* 749, 1995.

Sastry, T. S., Y. S. Sarma, S. V. S. Sarma, and P. V. Sanker Narayan, Day-time Pi pulsations at equatorial latitudes, *J. Atmos. Terr. Phys., 45,* 733, 1983.

Stuart, W. F., and H. G. Barsczus, Pi's observed in the daylight hemisphere at low latitudes, *J. Atmos. Terr. Phys.. 42,* 487, 1980.

Sugiura, M , and J. C. Cain, A model equatorial electrojet, *J. Geophys. Res., 71,* 1869, 1966.

Sugiura, M., and D. J. Poros, An improved model equatorial electrojet with a meridional current system, *J. Geophys. Res., 74,* 4025, 1969.

Sutcliffe, P. R., The longitudinal range of Pi 2 propagation at low latitudes, *Planet. Space Sci., 28,* 9, 1980.

Sutcliffe, P. R., and K. Yumoto, Dayside Pi 2 pulsations at low latitudes, *Geophys. Res. Lett., 16,* 887, 1989.

Tachihara, H., M. Shinohara, M. Shimoizumi, O. Saka, and T. Kitamura, Magnetometer system for studies of the equatorial electrojet and micropulsations in equatorial regions, *J. Geomagn. Geoelectr., 48,* 1311-1320, 1996.

Takahashi, K., S.-I. Ohtani, and K. Yumoto, AMPTE CCE observations of Pi 2 pulsations in the inner magnetosphere, *Geophys. Res. Lett., 19,* 1447, 1992.

Yumoto, K., and the 210° MM Magnetic Observation Group, The STEP 210° magnetic meridian network project, *J. Geomagn. Geoelectr., 48,* 1297-1309, 1996.

Yumoto, K., K. Takahashi, T. Sato, F. W. Menk, B. J. Frazer, T. A. Potemra, and L. J. Zanetti, Some aspects of the relation between Pi 1-2 magnetic pulsations observed at $L = 1.3$–2.1 on the ground and substorm-associated magnetic field variations in the near-Earth magnetotail observed by AMPTE CCE, *J. Geophys. Res., 94,* 3611, 1989.

Yumoto, K., K. Takahashi, T. Sakurai, P. R. Sutcliffe, S. Kokubun, H. Lühr, T. Saito, M. Kuwashima, and N. Sato, Multiple ground-based and satellite observations of global Pi 2 magnetic pulsations, *J. Geophys. Res., 95,* 15175, 1990.

Yumoto, K., et al., North/south asymmetry of sc/si magnetic variations observed along the 210° magnetic meridian, *J. Geomagn. Geoelectr., 48,* 1333-1340, 1996.

J. M. Da Costa and N. B. Trivedi, Instituto Nacional de Pesquisas Espaciais, C.P. 515, 12201-970, São José dos Campos, SP, Brazil.

N. Hosen, Hitachi Corporation, Hitachi, Ibaraki, Japan. T.-I. Kitamura, O. Saka, M. Shinohara, H. Tachihara, A. Yoshikawa, and K. Yumoto, Department of Earth and Planetary Sciences, Kyushu University, 33, Fukuoka, 812-81, Japan. (e-mail: shino@geo.kyushu-u.ac.jp)

N. J. Schuch, LACESM/CT, Universidade Federal de Santa Maria, CEP 97118-900, Santa Maria, RS, Brazil.

(Received November 4, 1996; revised October 17, 1997; accepted October 22, 1997.)